Definition of geohazards in exploration 3-D seismic data using attributes and neural-network analysis

Roar Heggland

ABSTRACT

During a geohazards evaluation of an area in deep-water Green Canyon, using standard exploration three-dimensional (3-D) seismic data, different features of significance to drilling operations and the planning of seabed installations were observed. These features were indications of seabed slope instability, shallow gas accumulations in a channel deposit, gas chimneys, faults, and a seabed mound above a gas chimney. Edge-detection maps were used to highlight slope-failure scars, faults, the channel, and the seabed mound. Average absolute-amplitude maps were used to highlight slope-failure scars, faults, and possible shallow gas accumulations. Possible gas chimneys were mapped to identify fluid-migration pathways. The mapping of chimneys was done by the use of a recently developed method for detection of gas chimneys in 3-D seismic data. The method was developed to facilitate and increase the consistency in the mapping, as well as make gas chimneys visible in the map view. The results of the geohazards assessment were identification of a seabed slope-failure risk and a risk of overpressured gas in channel deposits.

INTRODUCTION

This study is part of a geohazards assessment for an exploration well. The planned well location is in 2000 m (6600 ft) of water off the continental shelf in Green Canyon (Figure 1). The geohazards assessment is based on exploration three-dimensional (3-D) seismic data. This kind of assessment is done on a routine basis to avoid drilling problems, such as a gas blowout or subsidence of sediments in the well, causing loss of equipment and, in the worst case, loss of the drilling rig and human lives. In this paper, the results of the 3-D seismic interpretation will be presented, as well as a method for

Manuscript received December 3, 2001; revised manuscript received January 30, 2004; final acceptance February 4, 2004.

AUTHOR

ROAR HEGGLAND ~ *Statoil ASA, N-4035 Stavanger, Norway; rohe@statoil.com*

Roar Heggland is a geophysicist with Statoil ASA in Stavanger, Norway. He joined Statoil in 1984 and has worked as a seismic interpreter in exploration, research, and technology applications with specific focus on geohazards and fluid flow. He is coinventor of the method for detection of gas chimneys in 3-D seismic data. Roar Heggland holds a degree in particle physics from the University of Bergen, Norway.

ACKNOWLEDGEMENTS

Statoil ASA is acknowledged for giving permission to publish this article.

Figure 1. Location map.

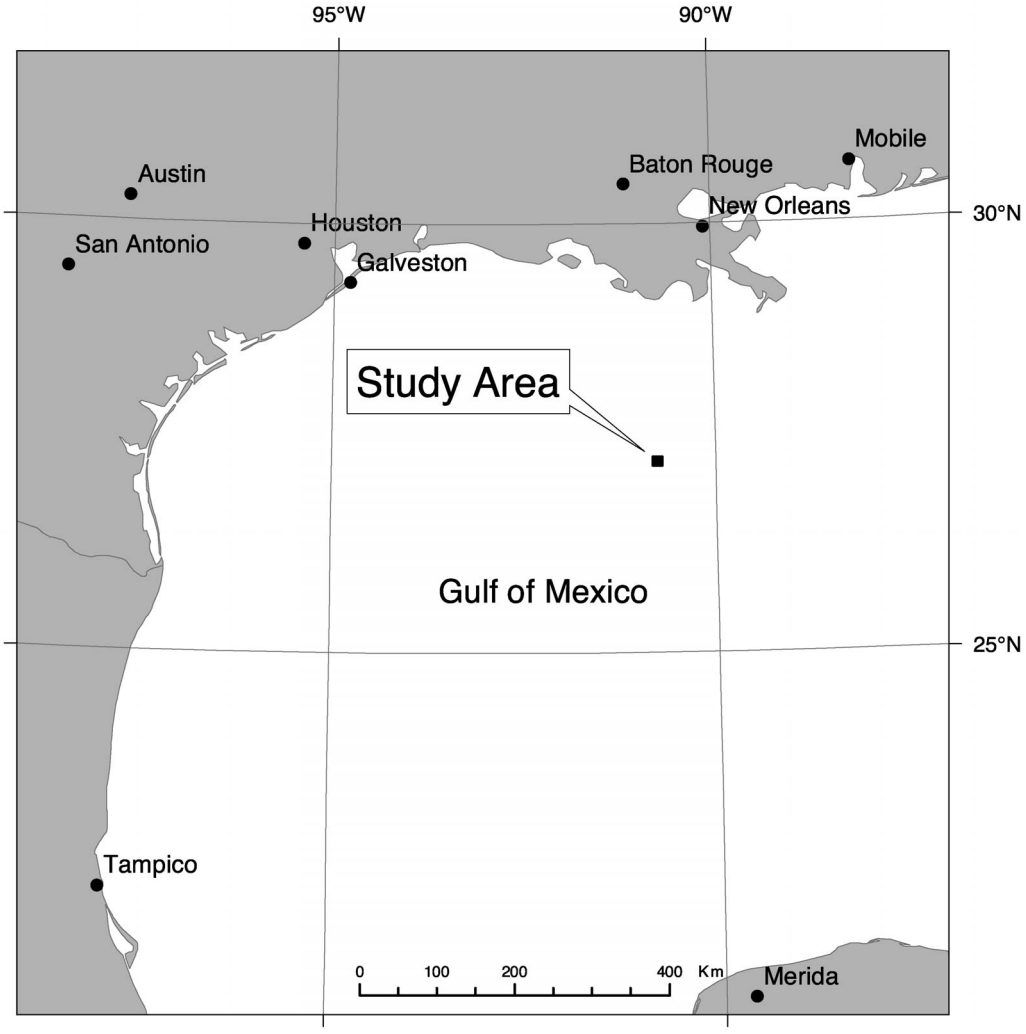

detection of gas chimneys in 3-D seismic data. Despite the fact that exploration 3-D data have a much lower vertical resolution than standard site survey (high-resolution) data, there is the advantage of having a much denser seismic line spacing, which enables the mapping of geological features that are not easily identified in two-dimensional data.

Within the area of investigation, uplift and faulting are believed to be caused by a salt dome. Three generations of slope failures are interpreted from the seismic data. The causes for the slope instabilities are believed to be a combination of the salt movement and high sedimentation rate. In the literature, different causes for slope instabilities have been proposed, such as uplift and faulting associated with salt intrusion (e.g., Cashman and Popenoe, 1985) or fluid escape and gas-hydrate dissociation (e.g., Quemeneur et al., 1995; Bryn et al., 1998; McNeill et al., 1998; Twichell and Cooper, 2000; Hovland et al., 2001).

High-amplitude anomalies are present at the base of a channel feature, indicating gas-charged deposits. Other high-amplitude anomalies, which may represent gas accumulations, are present in the study area, but were not regarded as hazards for drilling because either they were below the depth planned for drilling without a blowout preventer or they were defined as prospective targets. The upper sediments, normally from seabed down to between a few hundred meters and 1400 m (4600 ft), are drilled without a blowout preventer. This is because the blowout preventer is designed to fit on the second well casing, which is set at a depth in the interval mentioned.

The detected gas chimneys are located at faults near the top of the underlying dome structure. This is regarded as an indication that these faults are leaking. On top of a chimney reaching the seabed, a mound is present. The mound may be a mud volcano or a carbonate buildup, both of which can be associated with

the escape of gas. No seabed samples were taken at this stage of the investigation of the area to support the interpretation.

METHODS

Exploration 3-D seismic data, covering an area of 5 × 10 km (3 × 6 mi), were used for the mapping of geohazards. The data were acquired and processed using standard exploration 3-D seismic parameters. The inline spacing is 20 m (66 ft), the crossline spacing is 25 m (82 ft), and the sample rate is 4 ms. Three horizons, the seabed and two subsurface horizons, were mapped using a standard seismic interpretation software. To highlight features of interest, edge-detection and average absolute-amplitude maps were produced. Edge detection is a calculation of differences in dip across a horizon and highlights discontinuities on the horizon. The edge detection was applied on mapped time horizons to highlight steep dips, indicating escarpments and faults. The edge-detection values were displayed on top of the actual time horizon. Average absolute amplitude was calculated over time intervals parallel with and centered at the mapped subsurface horizons. The resulting amplitude values were displayed on top of the time horizons. The time window used was 40 ms two-way traveltime (TWT). The amplitude maps were used to identify amplitude anomalies representative of shallow gas accumulations, as well as identify faults and slope-failure scars. Faults and slope-failure scars stand out as low-amplitude features in the amplitude maps.

Because gas chimneys represent upward migration of gas, they can be used as indicators of gas charge of shallow reservoirs. If a gas chimney is identified close to a high-amplitude anomaly, it indicates a risk of a gas accumulation in a reservoir represented by the amplitude anomaly. Gas chimneys generally appear as diffuse columnar features in seismic data, taking various shapes, which can be very difficult to map manually. To facilitate and increase the consistency of the mapping of gas chimneys, a method has recently been developed for the detection of such features in 3-D seismic data (Heggland et al., 2000; Meldahl et al., 2001).

The first step in the chimney detection method is to make use of seismic attributes that enhance chimneys. The attributes that make the best contrast between chimneys and the surroundings are trace-to-trace similarity, amplitude (or energy), and time dip variance of seismic reflectors. A neural network (e.g., Steeghs, 1997; de Groot, 1999a, b) is trained by the use of these attributes at sample locations representing chimneys. The sample locations are chosen by the interpreter based on experience from interpreting chimneys. The neural network is also trained at nonchimney locations to recognize attribute values that are not representative of a chimney. A weighting function is applied to the seismic attributes. During training, the weighting function is adjusted to optimize the detection. Because chimneys appear as columnar disturbances in the seismic data, the detection process takes advantage of the vertical extents of chimneys using three vertically extended detection windows. In this way, features with similar seismic characteristics to chimneys but with minor vertical extents will be discriminated. The neural network performs this process at every sample location in the seismic volume. During the detection process, the network makes a classification of all data points into chimneys and nonchimneys. If the attribute values in all three windows are representative of being a chimney, a maximum value is assigned to the center sample in the middle window. The maximum value means a high probability that a chimney was detected. Likewise, a minimum value, meaning low probability, is assigned to the center sample if all three windows show attribute values that are not representative of a chimney. Because there also may be different attribute values in the three windows, the values in the output cube will not be limited to minimum and maximum numbers, but will have values ranging between minimum and maximum. The output data volumes are named chimney cubes.

RESULTS AND DISCUSSION

The potential geohazards identified in the 3-D data were a risk of seabed slope failure and possible gas-charged channel deposits. Mapping of gas chimneys and faults identify vertical fluid-migration pathways. One of the gas chimneys reaches the seabed and has a mound located on top of it. The mound is believed to be a small mud volcano or a carbonate buildup, both of which are commonly associated with gas escape to the seabed. Figure 2 shows a seismic section through the seabed mound. Based on the detection of gas chimneys, the mound was found to be located on top of a gas chimney. Mud volcanoes are commonly associated with gas escape and can release large amounts of mud and gas during eruptions (e.g., Guliev, 2003). Alternatively,

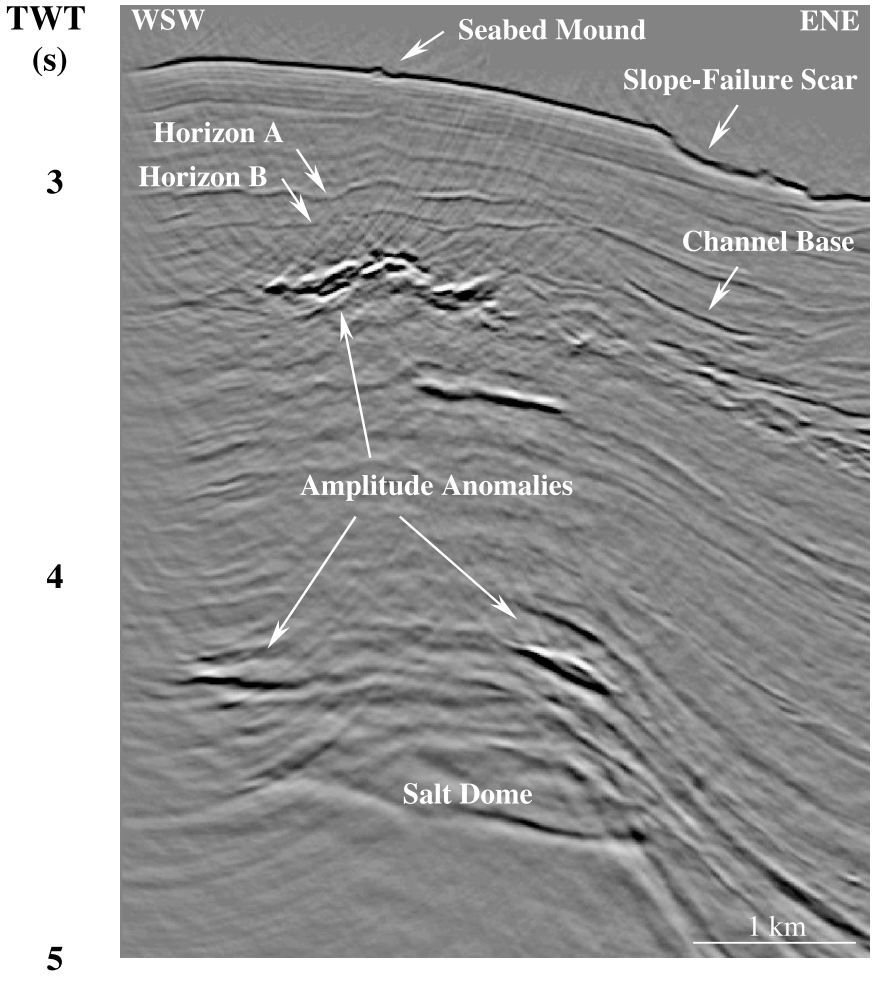

Figure 2. A 3-D seismic section from deep-water Green Canyon displaying the different features of interest in the geohazards evaluation. At the upper right, a seabed slope-failure scar can be seen. High-amplitude anomalies representing drilling prospects are indicated by arrows. Weak chimneys (see Figure 10) indicate migration of gas from the deep to the shallow prospect, as well as to the seabed, where a mound is present. A channel exhibits relatively high amplitudes at its base. This is more evident from the amplitude map in Figure 7. A salt dome can be seen in the lower section. Horizons A and B are indicated by arrows. Dark is positive amplitude, and light is negative.

representing a significantly slower process, carbonates can form mounds at gas-seepage locations (e.g., Hovland et al., 1994).

The seabed and two subseabed horizons, A and B, indicated in Figure 2, were mapped. A slope-failure scar, which has been interpreted at the seabed, and a channel exhibiting high amplitudes over a large part of its base, can be seen in Figure 2. The amplitude anomalies indicated in Figure 2 represent hydrocarbon drilling prospects.

Risk of Seabed Slope Failure

Features believed to be slope-failure scars were revealed during mapping of the seabed and the two subseabed horizons A and B. As indicated on the edge-detection map of the seabed in Figure 3b, a possible slope-failure scar is visible in the east middle part of the area. This is the same slope-failure scar that is indicated in the seismic section in Figure 2. The edge-detection map also shows a possible slope failure in the area to the west, as indicated in Figure 3b.

An edge-detection map of horizon A (Figure 4) shows two possible slope-failure scars and faults. An average absolute-amplitude map, using a 40-ms window centered at horizon A, shows that the possible slope-failure scars and faults are visible as low-amplitude (i.e., dark) areas (Figure 5).

Figure 6 shows an edge-detection map of horizon B, where another slope-failure scar, faults, and a channel are visible. An average absolute-amplitude map (Figure 7), using a 40-ms window centered at horizon B, shows the slope-failure scar and faults as low-amplitude areas and the channel base as a high-amplitude (light) feature. The relative positions of the scars on surfaces A and B (Figure 8) suggest that the failures are progressing upslope, and that another seabed slope failure may occur closer to the center of the dome structure. As mentioned above, the seabed edge-detection map in Figure 3 shows a possible slope failure in the area to

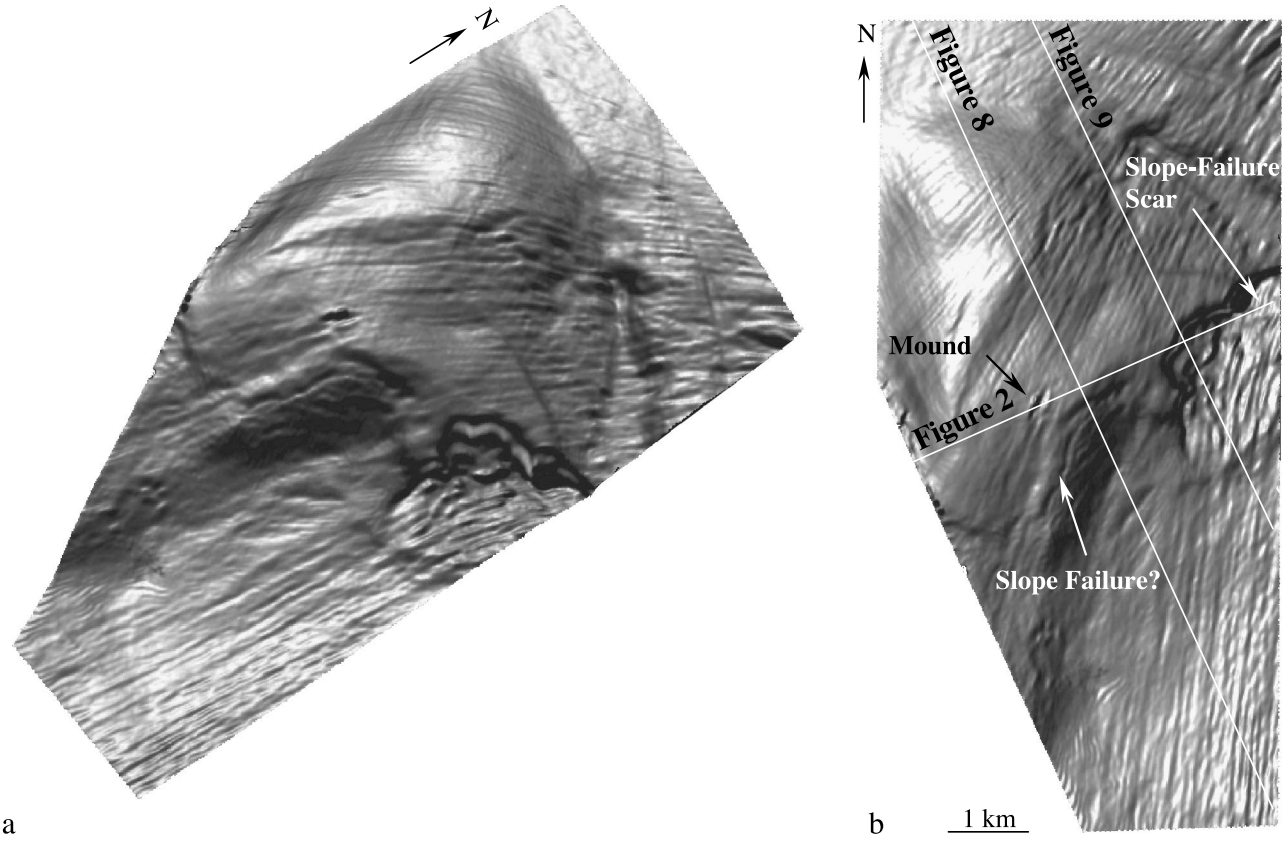

Figure 3. Edge-detection map of the seabed from 3-D seismic data, showing a slope-failure scar and an area with a risk of having a slope failure: (a) perspective view and (b) map view. A mound visible on the seabed is located above a chimney. Maximum dip is displayed in black and minimum dip in white.

the west. However, the seismic section in Figure 8, which goes across this feature, does not show a large scar at the seabed, like the section in Figure 2 does, in which case no mass seems to have moved down the slope yet. Because the two features look very similar on the seabed edge map, it is believed that there is a slope failure in its early phase in the area to the west. The position of the possible slope-failure feature is indicated in Figure 8, which shows that it is located closer to the center of the structure than the two previous slope failures at horizons A and B. This supports the hypothesis that a slope failure has already been initiated. Consequently, the area downdip of the slope-failure feature is regarded as not suited for drilling and seabed installations. Similar interpretations from off mid-Norway have been made by Bryn et al. (1998) and McNeill et al. (1998).

Gas-Charged Channel Deposits

The channel that was indicated in Figure 2 at horizon B, is evident from the edge-detection and amplitude maps in Figures 6 and 7. As mentioned in the introduction, the channel exhibits high amplitudes over large parts of its base. The high amplitudes may be caused by gas-charged deposits in the channel. Faults, visible as low amplitudes, are present across the channel.

A seismic section along the channel (Figure 9) shows that the faults have segmented the channel base into isolated compartments. If the faults and overlying sediments are impermeable, there is a potential for a pressure buildup in gas in the channel deposits. The gas-chimney detection shows no chimneys present at these faults, which could indicate gas leakage through the faults and an according pressure release. Drilling through the channel segments is therefore associated with a risk of encountering overpressured gas.

Detection of Gas Chimneys

As part of this investigation, gas chimneys were detected to evaluate vertical gas migration and charging

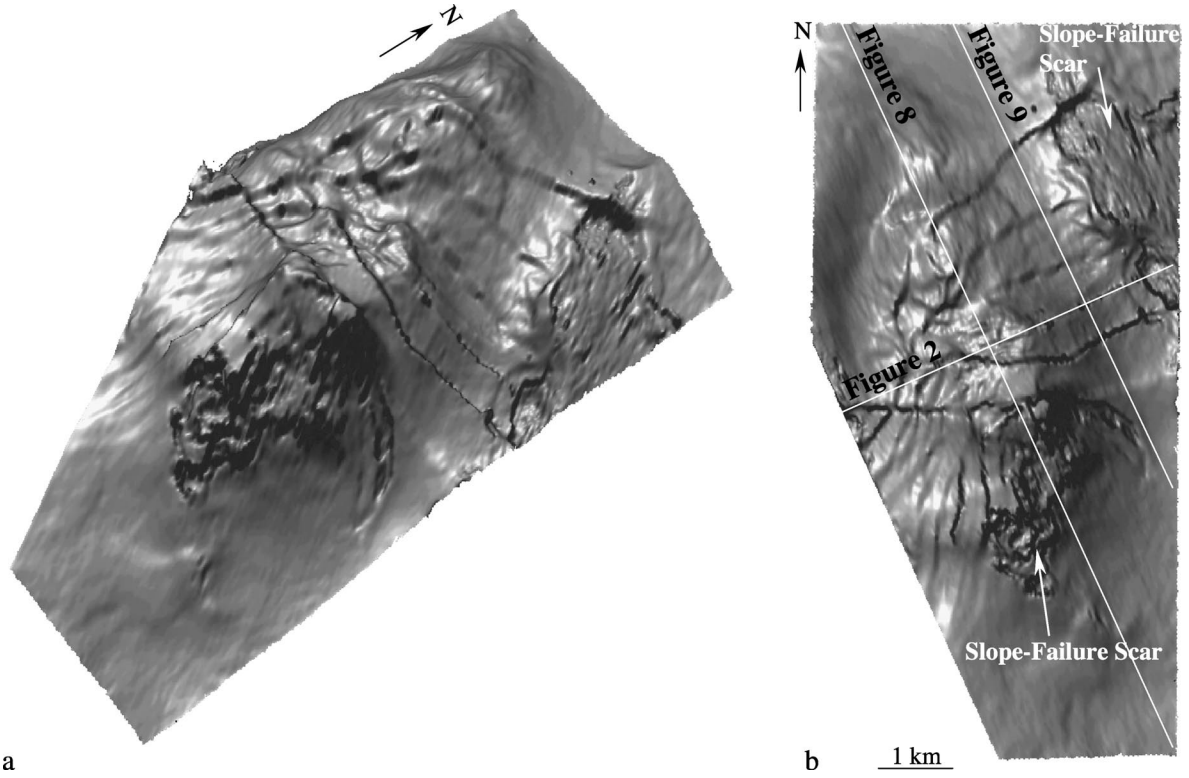

Figure 4. Edge-detection map of horizon A, exhibiting slope-failure scars and faults: (a) perspective view and (b) map view. Maximum dip is displayed in black and minimum dip in white.

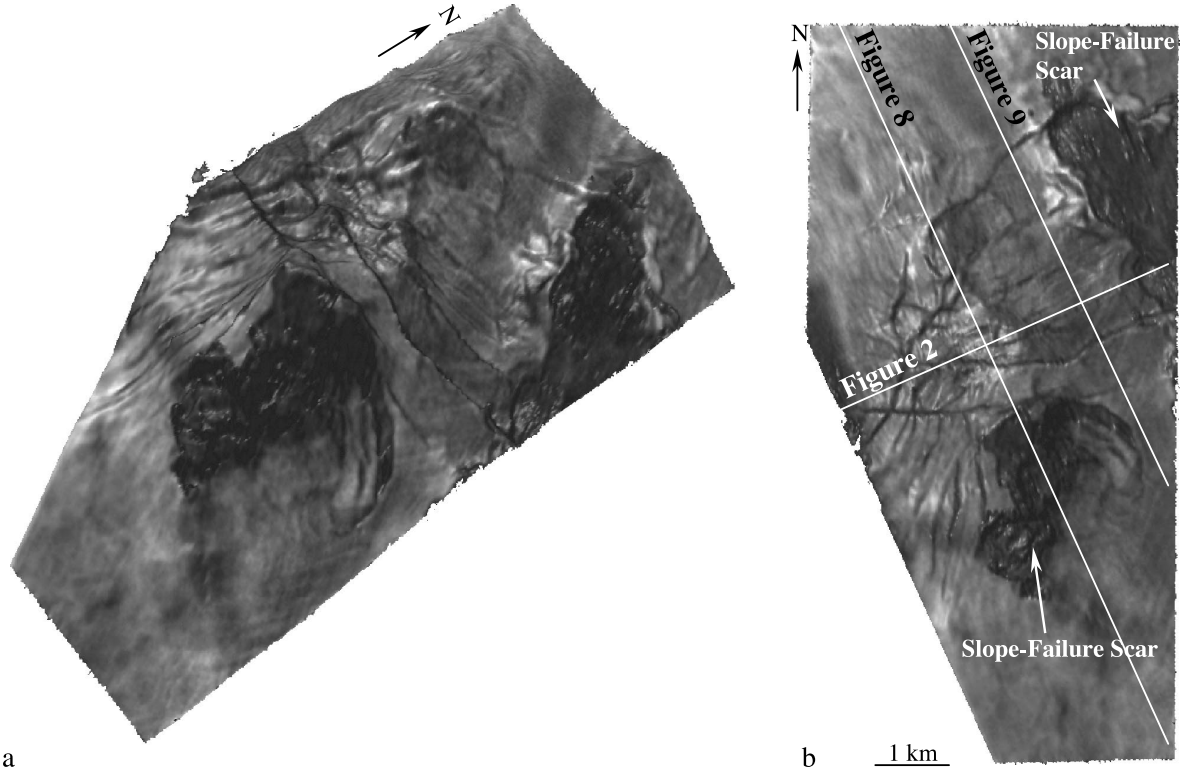

Figure 5. Average absolute amplitude over a 40-ms window centered at horizon A. Low-amplitude areas are dark, whereas high amplitudes are light. Slope-failure scars and faults are visible as low-amplitude areas (dark): (a) perspective view and (b) map view.

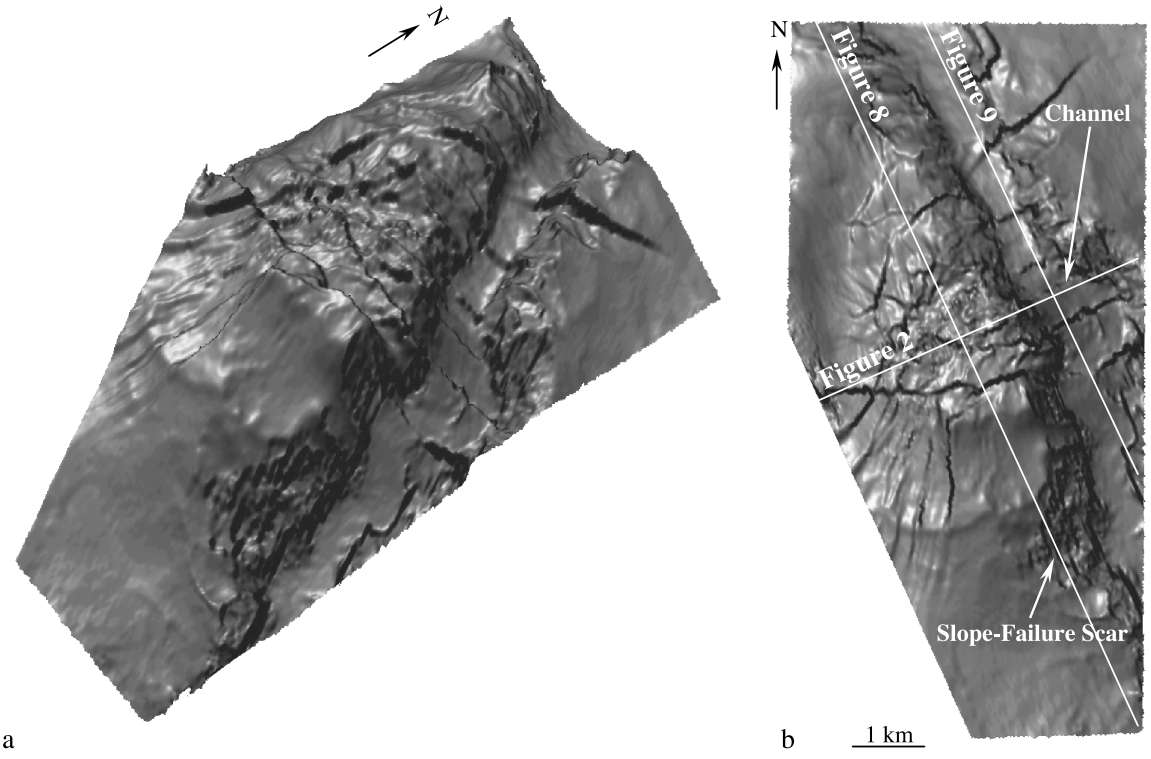

Figure 6. Edge-detection map of horizon B, showing a slope-failure scar, faults, and a channel: (a) perspective view and (b) map view. Maximum dip is displayed in black and minimum dip in white.

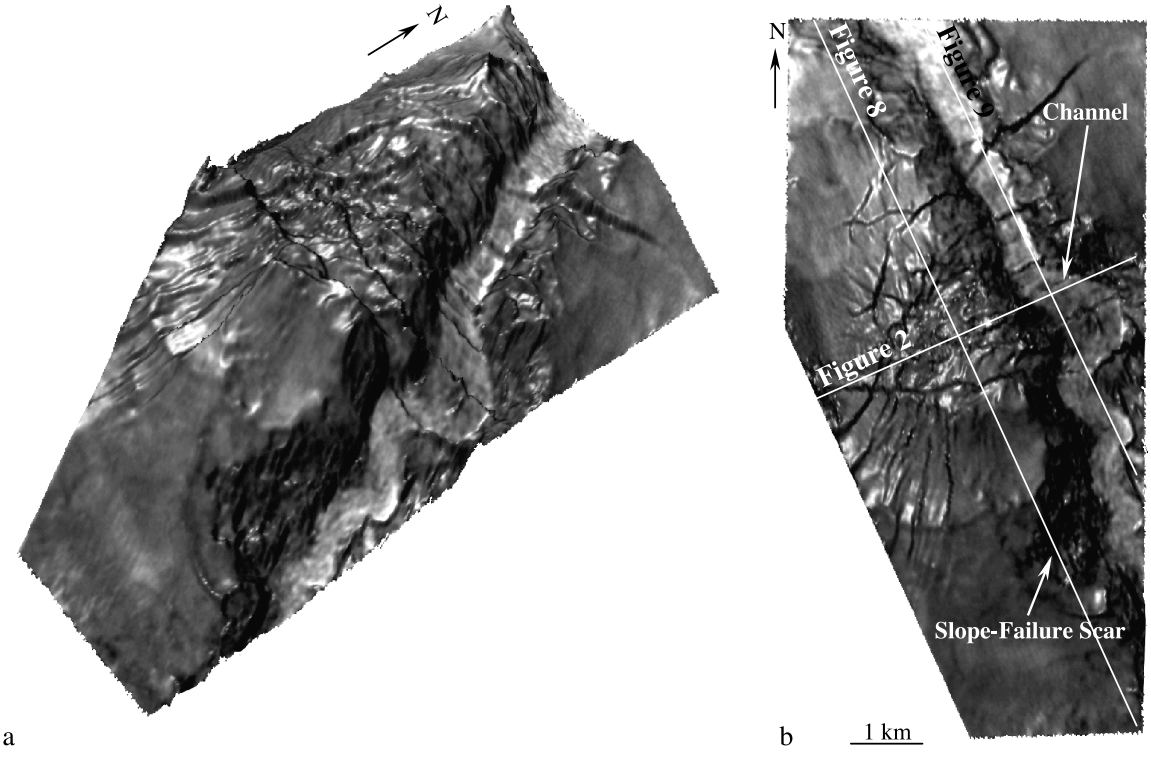

Figure 7. Average absolute amplitude over a 40-ms window centered at horizon B. Low-amplitude areas are dark, whereas high amplitudes are light. A slope-failure scar and faults are visible as low-amplitude areas (dark). A channel is visible as a high-amplitude feature (light): (a) perspective view and (b) map view.

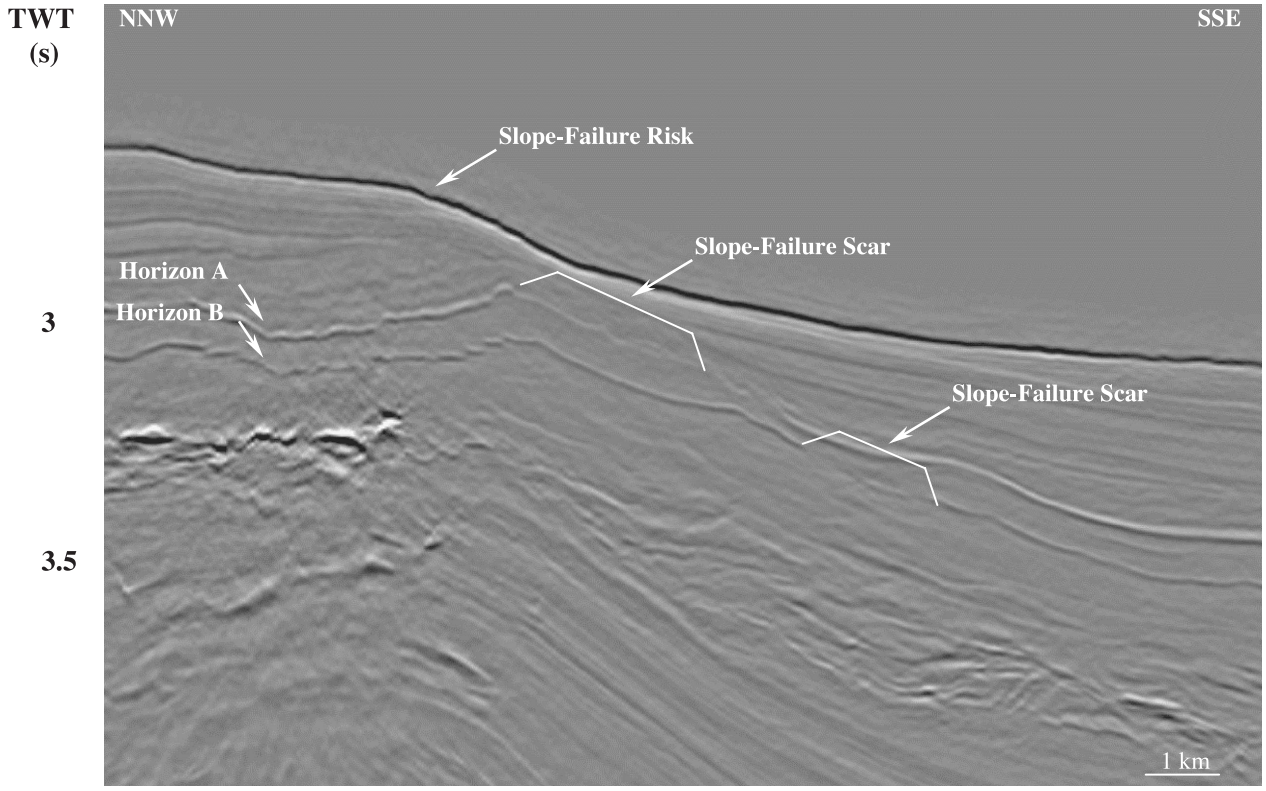

Figure 8. A 3-D seismic section showing the relative positions of slope-failure scars at horizons A and B and the location at the seabed where a slope-failure risk may be present (see also Figure 3). Dark is positive amplitudes, and light is negative.

Figure 9. A 3-D seismic section along the channel in Figure 8. The channel has been segmented by faults. The slope-failure scar at the seabed is the same as can be seen in Figure 2. Dark is positive amplitudes, and light is negative.

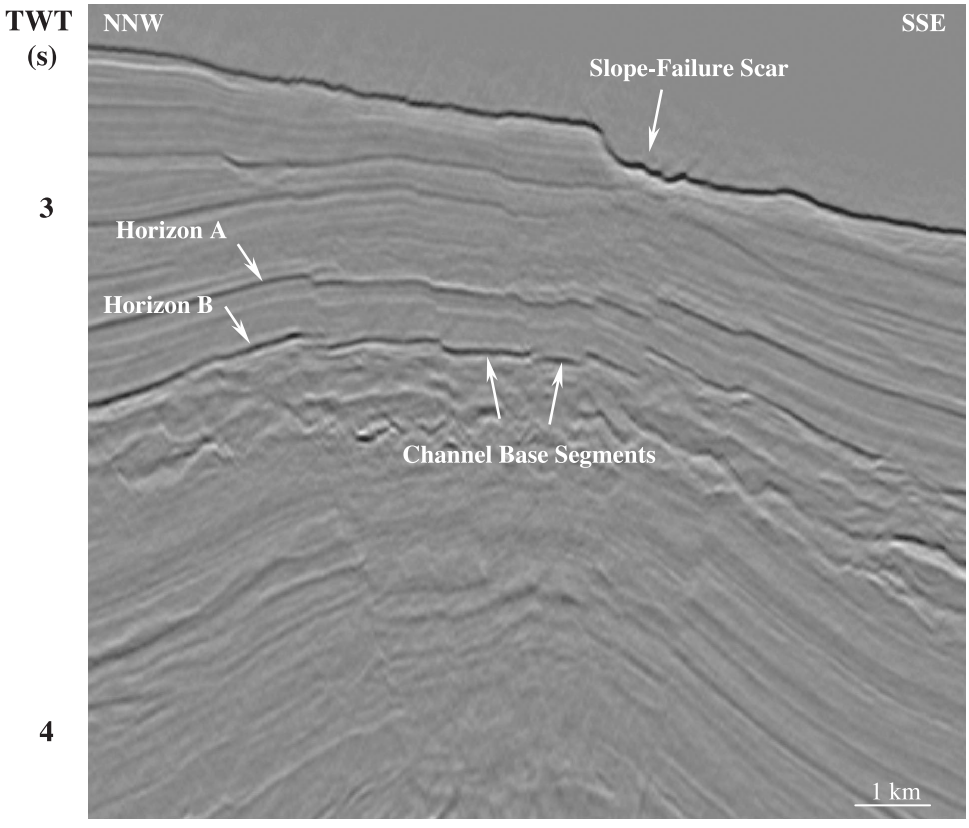

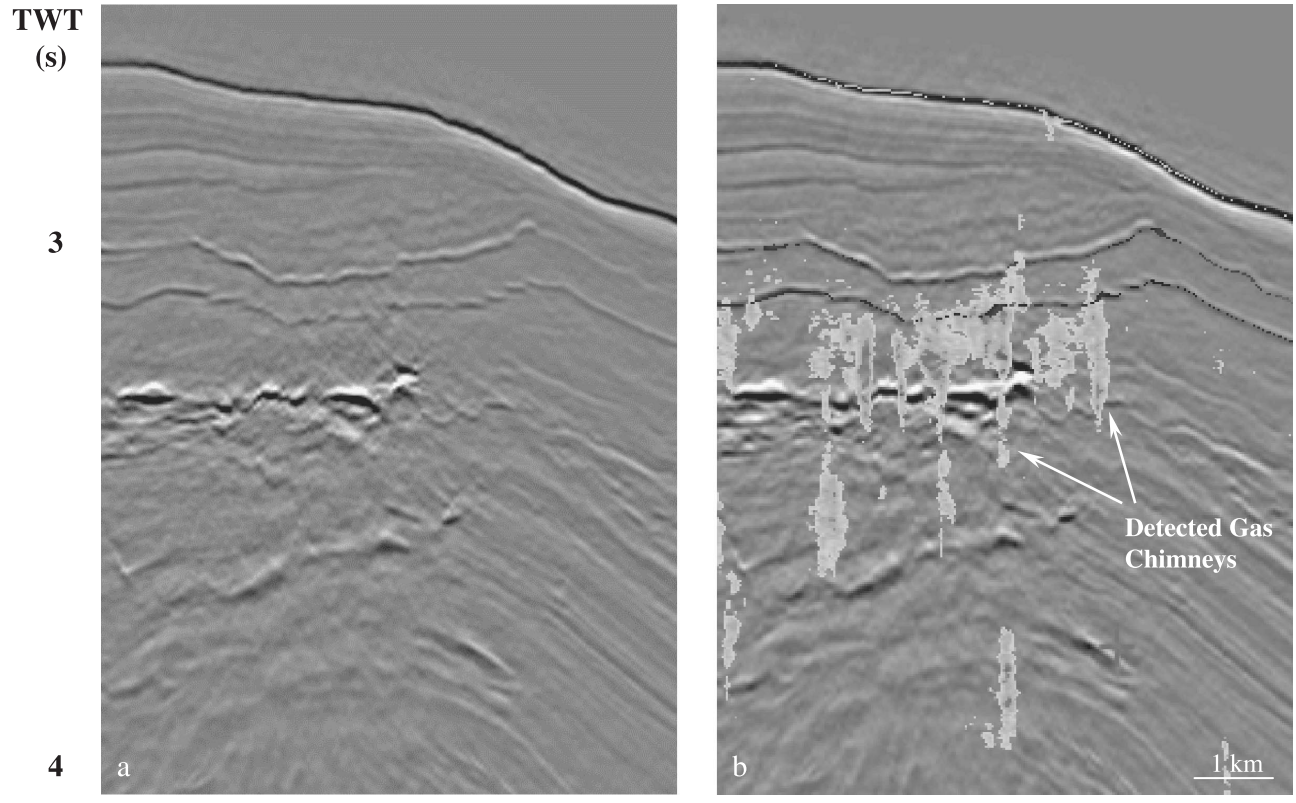

Figure 10. Part of the 3-D seismic section in Figure 9, (a) without detected gas chimneys displayed and (b) with detected gas chimneys displayed.

of shallow reservoirs (Heggland 1997, 1998). Figure 10 shows a seismic section across the dome with and without detected chimneys displayed on it.

Because of the separation of the data in a chimney cube into high and low values, the detected chimneys can easily be visualized by making the surrounding volume (represented by the low values) transparent. In Figure 11, the chimney cube is presented in this way (Heggland et al., 2000). The chimneys (yellow) have been displayed together with the three mapped horizons, the seabed (brown), horizon A (green), and horizon B (blue). High amplitudes (red) from the standard 3-D data have been displayed in the same manner as the chimney cube. The high amplitudes outline two possibly hydrocarbon-charged reservoirs. The salt dome (white bluish) has been detected using a modified version of the chimney detection method and has been visualized in the same way as the chimneys.

The chimneys indicate upward migration of gas from the deep to the shallow prospect. Figure 12a and b show detected chimneys displayed together with the average absolute-amplitude maps centered at horizons A and B, where it can be seen that the chimneys line up with faults. Shallow faults across the highest part of the structure have gas chimneys associated with them, which could mean that gas migrates to the seabed. If gas is present in the shallow reservoir, overpressure is not expected because the gas is believed to be flowing through. The presence of gas chimneys at a fault is believed to be caused by present or previous leakage through the fault. The gas chimneys can be generated by gas coming out of solution from water moving up the fault, in which case the open fault can also be or have been a migration pathway for free gas as well as oil.

CONCLUSIONS

The principal geohazards identified in this study were found to be a risk of slope failure and risk of overpressured gas accumulations in a channel deposit. Edge-detection maps were found to be useful for the study of the shape of the horizons to identify mounds, depressions, faults, and channels. Average absolute-amplitude maps were used for the mapping of high-amplitude

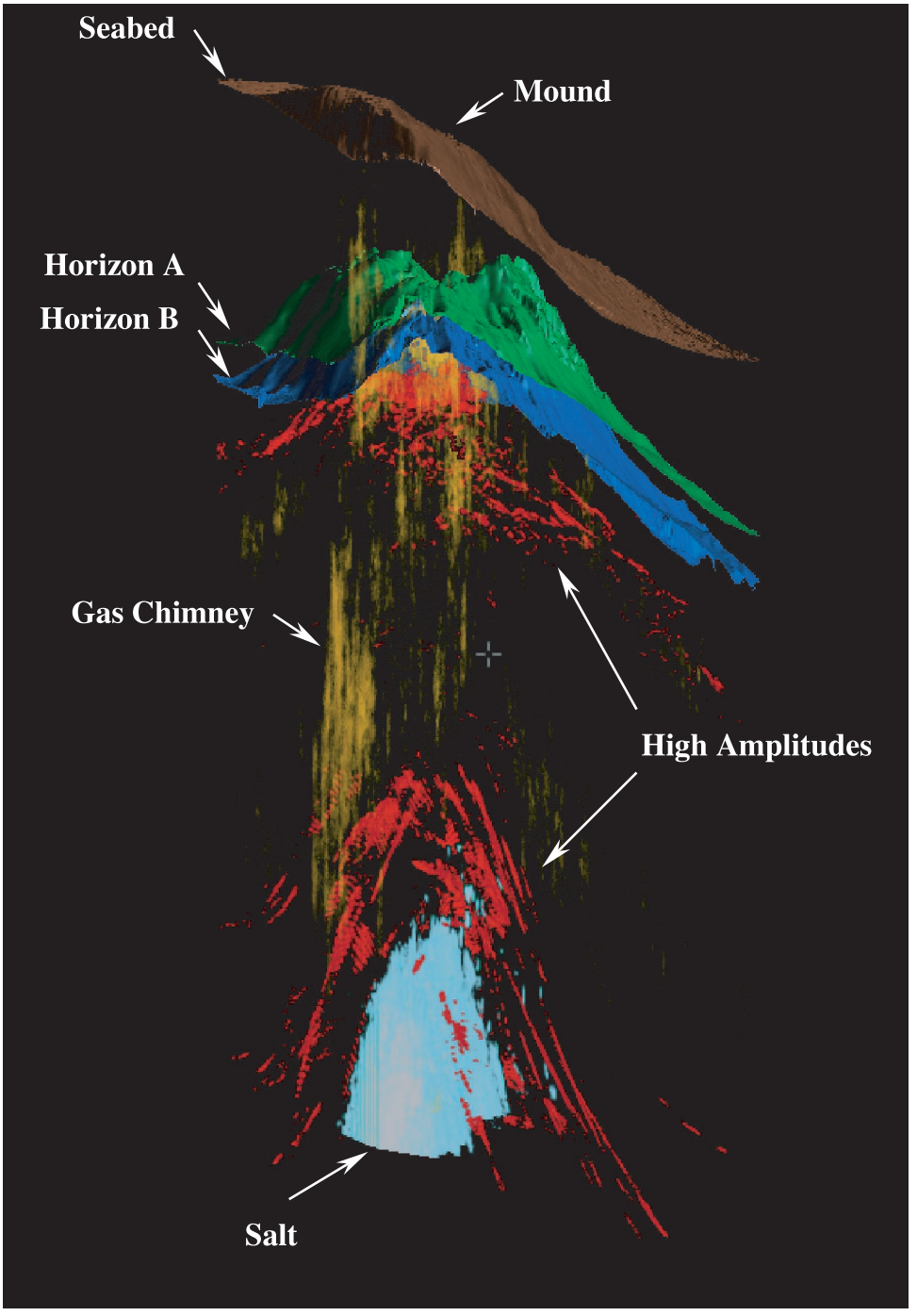

Figure 11. Three-dimensional visualization showing mapped seabed (brown), horizon A (green) and horizon B (blue). High amplitudes in red outline a shallow and a deep prospect. A salt diapir at the base has been detected and displayed in white-bluish color. Detected gas chimneys are displayed in yellow and indicate migration of gas from the deep prospect to the shallow prospect and further to the seabed.

anomalies to predict shallow gas accumulations. Average absolute-amplitude maps were also well suited for the mapping of faults and slope-failure scars, visible as low-amplitude features.

Application of a method designed for detection of chimneys in 3-D seismic data has made it possible to map chimneys that otherwise would have been very difficult to identify. The benefits of mapping gas chimneys are as follows: they can indicate fluid-migration pathways and show where gas accumulations are likely to be present, as they can indicate charging of reservoirs from a deeper level. Gas chimneys lining up with faults above a possible reservoir indicated leakage and a probable pressure release. Absence of chimneys along faults across a possible gas-charged channel sand may indicate risk of overpressure.

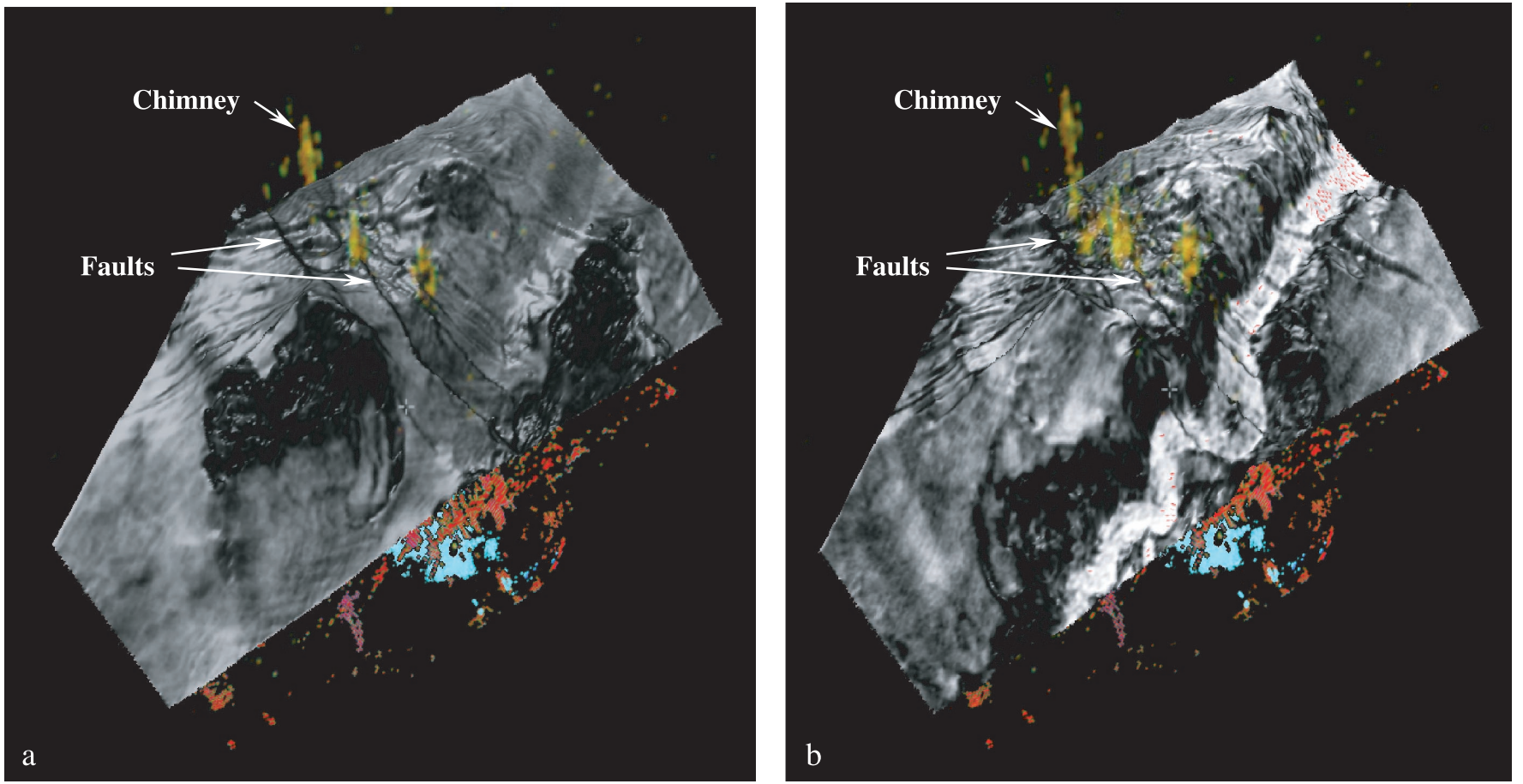

Figure 12. Three-dimensional visualizations showing (a) average absolute-amplitude map over a 40-ms window centered at horizon A and detected chimneys in yellow, (b) average absolute amplitude over a 40-ms window centered at horizon B. Low-amplitude areas are dark, whereas high amplitudes are light. The detected gas chimneys line up with faults, indicating that the faults are leaking.

REFERENCES CITED

Bryn, P., S. R. Østmo, R. Lien, K. Berg, and T. I. Tjelta, 1998, Slope stability in the deep water areas off mid-Norway: Offshore Technology Conference, Houston, May 4–7.

Cashman, K. V., and P. Popenoe, 1985, Slumping and shallow faulting related to the presence of salt on the continental slope and rise off North Carolina: Marine and Petroleum Geology, v. 2, p. 260–271.

de Groot, P. F. M., 1999a, Seismic reservoir characterisation using artificial neural networks: 19th Mintrop-Seminar, May 16–18, 1999, Münster, Germany.

de Groot, P. F. M., 1999b, Volume transformation by way of neural network mapping: 61st European Association of Geoscientists and Engineers Conference, Helsinki, June 7–11, 1999.

Guliev, I., 2003, The south Caspian Basin— Excitement and movement of sedimentary masses: Mechanism and geologic consequences (abs.): AAPG Annual Meeting, Salt Lake City, Utah, May 11–14.

Heggland, R., 1997, Detection of gas migration from a deep source by the use of exploration 3-D seismic data: Marine Geology, v. 137, p. 41–47.

Heggland, R., 1998, Gas seepage as an indicator of deeper prospective reservoirs. A study based on exploration 3-D seismic data: Marine and Petroleum Geology, v. 15, p. 1–9.

Heggland, R., P. Meldahl, P. de Groot, and F. Aminzadeh, 2000, Chimneys in the Gulf of Mexico: The American Oil and Gas Reporter, February 2000, p. 78–83.

Hovland, M., P. F. Croker, and M. Martin, 1994, Fault-associated seabed mounds (carbonate knolls?) off western Ireland and north-west Australia: Marine and Petroleum Geology, v. 11, p. 232–246.

Hovland, M., P. A. Bjørkum, O. T. Gudmestad, and D. Orange, 2001, Gas hydrate and seeps— Effects on slope stability: The ''hydraulic model:'' 11th International Society of Offshore and Polar Engineers et al. Conference Proceedings, v. 1, p. 471–476.

McNeill, A. E., R. S. K. Salisbury, S. R. Østmo, R. Lien, and D. Evans, 1998, A regional shallow stratigraphic framework off mid-Norway and observations of deep water ''special features'': Offshore Technology Conference Proceedings, v. 1, p. 97–109.

Meldahl, P., R. Heggland, B. Bril, and P. de Groot, 2001, Identifying faults and gas chimneys using multi attributes and neural networks: The Leading Edge, May 2001, p. 474–482.

Quemeneur, P., J. P. Tisot, P. Cochonat, J. F. Bourillet, V. D'oultremont, J. L. Colliat, and R. Tofani, 1995, Potential causes for slope instabilities of under-consolidated marine sediments: 5th International Society of Offshore and Polar Engineers et al. Conference Proceedings, v. 1, p. 448–453.

Steeghs, T. P. H., 1997, Local power spectra and seismic interpretation: Ph.D. thesis, Section for Applied Geophysics, Faculty of Applied Earth Sciences, Delft University of Technology, ISBN 90-90108 12-2.

Twichell D. C., and A. K. Cooper, 2000, Relation between seafloor failures and gas hydrates in the Gulf of Mexico, A regional comparison (abs.): AAPG-SEPM Annual Convention Program, v. 9, p. A150.